Characterization of Fluor Concentration and Geometry in Organic Scintillators for *in Situ* Beta Imaging

Martin P. Tornai, Edward J. Hoffman, *Senior Member, IEEE,*
Lawrence R. MacDonald, and Craig S. Levin, *Member, IEEE*

***Abstract*—Development of a small area (1–2 cm^2) *in situ* beta imaging device includes optimization of the front end scintillation detector, which is fiber optically coupled to a remote photon detector. Thin plastic scintillation detectors, which are sensitive to charged particles, are the ideal detectors due to the low sensitivity to ambient gamma backgrounds. The light output of a new binary plastic scintillator was investigated with respect to increasing concentrations of the fluor (0.5–2.0% by weight) and varying thickness cylindrical configurations of the intended imaging detector. The fluor had an emission maximum increasing from 431 to 436 nm with increasing fluor concentration. The decay time(s) had two components (0.38 and 1.74 ns). There was an ∼20% increase in light output with increasing fluor concentration, measured with both ^{204}Tl betas and conversion electrons from ^{207}Bi. The highest light output of this new scintillator was measured to be ∼30% lower than BC404. Simulations predicted the 1.5 mm scintillator thickness at which light output and energy absorption for ∼700 keV electrons (e.g., from ^{204}Tl, ^{18}F) were maximized, which corresponded with measurements. As beta continua are relatively featureless, energy calibration for the thin scintillators was investigated using Landau distributions, which appear as distinct peaks in the spectra. As the scintillators were made thinner, gamma backgrounds were shown to linearly decrease.**

I. Introduction

DEVELOPMENT of a small area (1–2 cm^2) *in situ* beta detecting and imaging device for surgical resection of residual $\beta\pm$ radiolabeled tumor deposits includes optimization of the front-end scintillation detector, which is fiber optically coupled to a remote photon detector (Fig. 1, [1]–[5]). The probe front end is a scintillator coupled to flexible optical fibers, which keep all electrical components far from the surgical cavity. Gamma transparent materials are necessary to avoid detection and consequent image misposition due to ambient gamma backgrounds (e.g., annihilation photons from ^{18}F positrons).

The success of the imaging device depends on detecting a sufficient number of optical photons at the photodetector end [6] with which energy and positioning information combine to form images of the beta distributions. A high photon yield plastic scintillation detector that is sensitive to charged particles ($\beta\pm$) of <1 MeV would be the ideal detector due to its low Z (6.6) and density (1.05 g/cm^3), hence low sensitivity to ambient gamma backgrounds. Organic scintillators have a known variation in light output and decay time as a function of fluor (dopant) concentration [7], [8]. Additionally, optimization of scintillator geometry is an important aspect of maximizing pulse height, especially when guiding light into and through fiber optics [1]–[5]. In this work, a binary fluor (from Bicron) prepared in various high concentrations (0.5–2.0% by weight) in a polyvinyltoluene (PVT) solvent matrix was evaluated in comparison to commercially available BC404 (Bicron) to determine its suitability for use in the beta imaging probe. Various geometrical conditions necessary for optimal light output and device operation were also investigated by simulations and measurements.

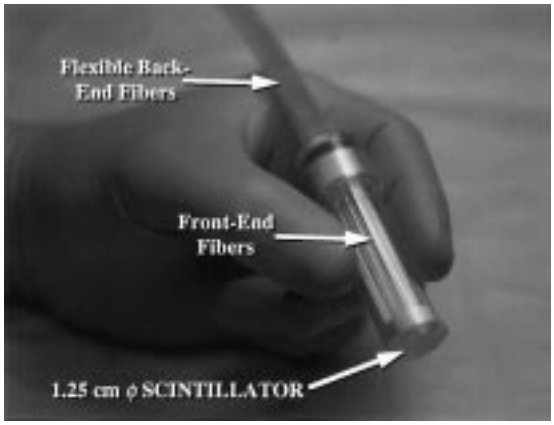

Fig. 1. Photograph of the intra-operative imaging device.

II. Materials and Methods

Samples of the new plastic scintillator were prepared by Bicron (Newbury, OH) to our specifications from 0.5 to 2.0% concentration by weight, in 0.25% steps, in a PVT matrix. The samples were 1.74 cm in diameter $(\phi)x \sim 5$ mm thick and had a visibly high quality polish on all surfaces.

Spectrophotometric analysis of the 0.05% dilute, pure fluor (CH_3–C_6H_4CH=CH_2–C_6H_4) was performed at Bicron. The spectral emission of the plastic scintillator samples was mea-

Manuscript received December 1, 1995. This work was supported in part by DOE contract DE-FC03-87-ER60615 and NCI grant R01-CA61037.

M. P. Tornai, E. J. Hoffman, and C. S. Levin are with the Division of Nuclear Medicine and Biophysics, Department of Molecular and Medical Pharmacology, University of California at Los Angeles School of Medicine, Los Angeles, CA 90095 USA.

L. R. MacDonald is with the Department of Physics, University of California at Los Angeles, Los Angeles, CA 90095 USA.

Publisher Item Identifier S 0018-9499(96)08975-7.

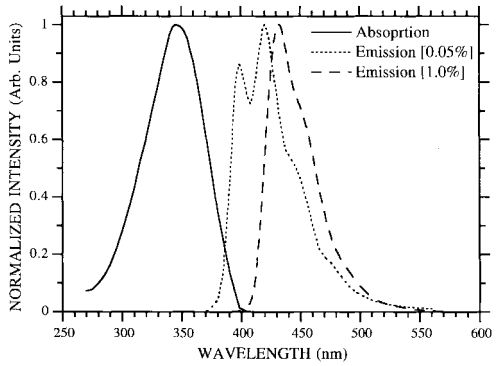

Fig. 2. Emission spectra of a highly diluted (0.05%), pure sample in solution, and 1.0% fluor sample in PVT matrix, i.e., plastic scintillator form.

sured at the University of California at Los Angeles (UCLA) on a Perkin–Elmer Luminescent Spectrophotometer with a spectrally calibrated EMI 9781 PMT. The samples were irradiated at the maximum absorption wavelength (see Fig. 2) and read out 90° with respect to the collimated excitation beam.

The decay time measurement method utilized a modified Bollinger and Thomas technique [9] with single photoelectron (PE) method [10], [11]. Two RCA C31024 PMT's with <200 ps time resolution [12] were used in coincidence, with the first (TAC Start) triggering on the prompt ($\gg$1 PE) signal and the second (TAC Stop) triggering at the single PE level.

Light yield measurements were made with the cylindrical pieces, highly polished on the side and PMT contact surface, and lightly ground (60 μm granularity) opposite the PMT. The pieces were covered with a thin layer of Teflon and optically coupled ($n_{\text{grease}} = 1.49$) to a calibrated C31024 PMT. These measurements were made at several thicknesses for each scintillator. The samples were uniformly irradiated with the conversion electrons from ^{207}Bi ($E_{\text{IC}\,e-} = 976$ keV, $E_{\text{IC}\,e-} =$ 482 keV) and the beta continuum of ^{204}Tl ($E_{\beta\,\max} = 763$ keV, $E_{\beta\,\text{avg}} = 254$ keV) in an aluminum dark box. ^{204}Tl is a pure β^- emitter with similar energy to β^+ in ^{18}F ($E_{\beta\,\max} = 635$ keV), an intended radioisotope for use with the imaging device. ^{204}Tl betas are without the corresponding annihilation photons, facilitating measurements during device optimization. The centroid of the gamma background subtracted conversion electron spectra (Gaussian fit) and weighted mean of the beta continua were calculated from the measurements as a measure of the pulse height.

Monte Carlo simulations were performed on code developed at UCLA to track electron trajectories and tally energy deposition in various materials [5]. Simulated monoenergetic electrons from ^{207}Bi and ^{204}Tl betas flood irradiated (200 000 electrons per condition, normal incidence) the 1.25 cm ϕ and various thickness (0.5–5.0 mm) plastic ($Z_{eff} = 6.6$, $\rho = 1.05$ gm/cm^3) disks. The light output for similar geometry scintillators with various surface treatments was simulated with optical photon tracking using DETECT [13]. The same number of photons (100 000) were uniformly generated in each size and surface treated disk. All disks had diffuse, absorbing sides, conditions that are known to improve positioning accuracy at the edges of continuous positioning detectors [4], e.g., in gamma cameras. Various front surface treatments were investigated for the scintillator incorporated in the imaging device because: 1) ambient light external to the scintillator must be shielded so that the detector signal will not be corrupted; and 2) the thin ambient light shield has a reflective inner surface to direct photons back toward and into the optical fibers.

The gamma background from ^{207}Bi was measured in the scintillators by shielding the detectors with a 1-cm-thick black PMMA block. The higher energy gamma component (1063 keV) was subtracted from the total background, leaving the background component due to the lower energy gammas only (569 keV). The integral events in the remaining distribution thus represent the gamma contribution from near 511 keV gammas, as 511 keV gammas are expected from positron annihilation from ^{18}F radiolabels. The integral events were then normalized to the thickest (5 mm) scintillators used in the measurements.

III. Results

A. Spectral Characteristics

The maximum absorption and emission wavelengths for the dilute (0.05%) fluor sample were found to be 347 and 420 nm, respectively (Fig. 2). The molar extinction coefficient was determined to be ~57 000 l/mol-cm. The emission maxima for the various concentration (0.5%–2.0%) samples systematically increased from 431 to 436 nm. The 1.0% fluor sample had a 433 nm maximum (Fig. 2). With higher concentrations of dopant, self-absorption of shorter wavelength light increases, as expected [7], raising the maximum emission wavelength and potentially leading to shorter attenuation lengths in the bulk scintillator. Because we anticipate using thin scintillators (0.5–3 mm) in the imaging device, attenuation factors do not play as great a role as other factors, e.g., intrinsic scintillation. The new scintillator shows a good spectral match with absorption in bialkali photocathode PMT's.

B. Decay Time

The decay time of the 1.0% scintillator sample was measured and compared with a BC404 standard (Fig. 3). The corrected decay times for the 1.0% sample were found to be 0.38 and 1.74 ns, while the decay time of BC404 was measured to be 1.2 ns.

The first peak in the 1.0% sample time spectra may be due to increased Förster transitions (direct fluor excitation) with high concentration of dopant, and the second from solvent (PVT) radiative transfer to the fluor. With lower concentrations, lower intensity first peaks might be expected. With higher concentrations of fluor an increase in the first peak intensity is expected as the direct excitation probability increases. This is consistent with known decreasing decay times as fluor concentration increases in liquid scintillators [7]. The first peak may also be due to prompt Cerenkov light produced above the ~150-keV threshold in PVT ($n = 1.58$), although this effect is not seen in the BC404 sample. Similar peaks in timing spectra have been observed for high dopant concentrations in plastic scintillators [8].

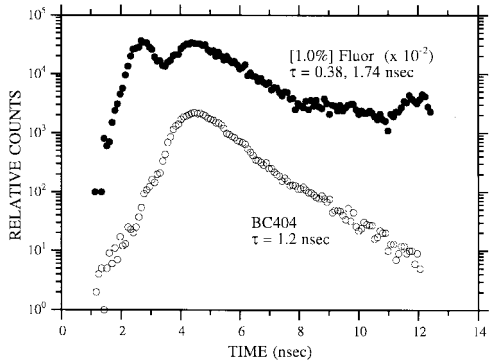

Fig. 3. The new (1.0%) scintillator decay time compared to standard BC404. Long decay times were derived from exponential fits to data; the short decay time was corrected for build-up of the slower component.

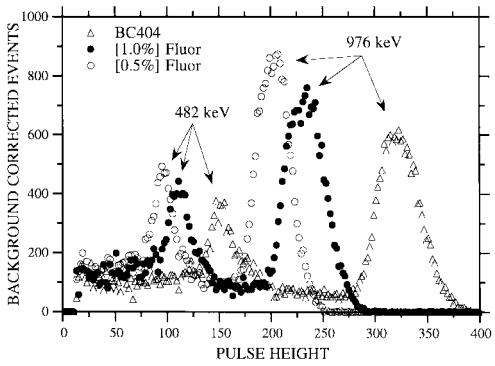

Fig. 4. ^{207}Bi conversion electron (gamma background subtracted) energy spectra for two concentrations of the new plastic scintillator compared with BC404. The scintillators had similar geometries and surface treatments.

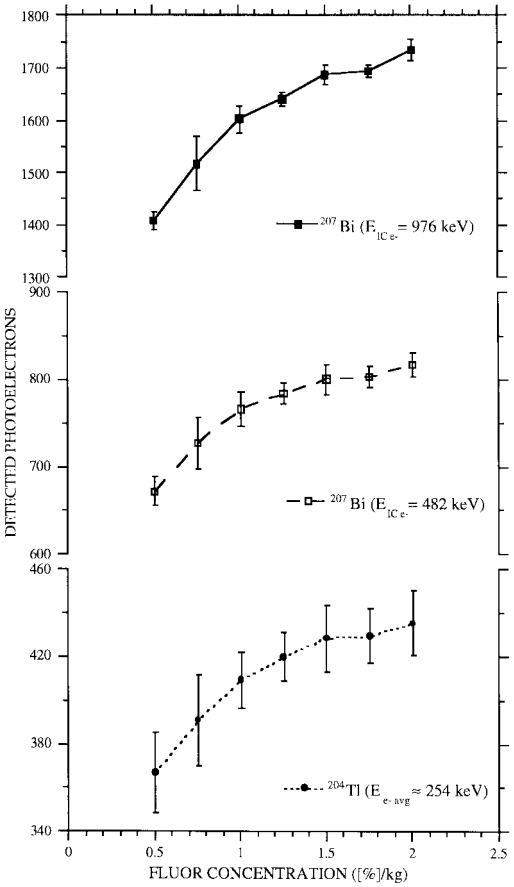

Fig. 5. Measured light yields for the new plastic scintillators as a function of increasing fluor concentration, irradiated with ^{207}Bi conversion electrons and ^{204}Tl betas. Error bars are for multiple measurements.

C. Concentration Effects

Energy spectra with ^{207}Bi demonstrated a distinct variation in pulse height between the scintillators (Fig. 4). There was an ~20% improvement in light yield from lowest to highest concentration doping of the new plastic scintillator, with the first ~13% improvement from 0.5% to 1.0% and an incremental increase thereafter (Fig. 5). The highest yield mixture, 2.0% fluor, was still 30% lower in light output than a similar sample of BC404 scintillator.

There was a reasonable correspondence (±17%) of the relative changes in light yield measured with ^{207}Bi conversion electrons and ^{204}Tl betas in the different concentration samples. This result indicates that in low light situations the weighted means of beta continua are good indications of pulse height. In low light level situations, e.g., signals from plastic scintillators through 2 m of optical fibers as intended in the beta imaging device, spectral energy distributions tend to be featureless and energy calibration of devices is more difficult. For thin scintillators (see Section III-F), degradation of features is more pronounced, and thus centroid weighting on beta continua may be one method for device calibration.

D. Simulation Results

The total absorption probability is defined as the probability of absorbing all incident electron energy in the target material [5]. Due to surface backscatter and side scatter out from the sides of the cylinder, the total absorption probability, even for large disks, never reaches 1.0.

Too thin a scintillator compromises the ability to detect all the beta energy, and hence leads to degraded scintillation light signal. Large disk scintillators would have expectedly higher contributions from ambient gamma backgrounds (see Section III-F). The simulations predict that for decreasing thicknesses of plastic scintillators, 90% absorption is achieved for 482 keV electrons with ~2.0-mm-thick disks (Fig. 6). The calculated range for maximum energy ^{18}F positrons is ~2.2 mm and ~0.68 mm for average energy ^{18}F positrons. These simulations and calculation results predict that optimum thicknesses for 1.25 cm ϕ plastic scintillators in this imaging application should be between 0.5–2.5 mm at these electron energies. These values agree with other measurements [5].

Note that from the optical tracking simulations, decreasing scintillator thickness corresponds to higher light output in all surface treatment cases (Fig. 7). This result is consistent with the collection of greater numbers of photons with improved solid angle to the detector [4], [5], in this case facilitated by thinner disks. The ideal scintillator will be a compromise between electron energy absorption and light yield (which includes scintillator geometry) in an attempt to maximize light output (see Fig. 9) from thin scintillators coupled through fiber optics to the photon detector(s) [5].

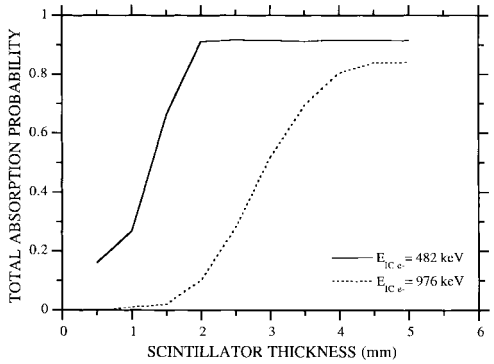

Fig. 6. ^{207}Bi conversion electron energy deposition simulation results. Note that total absorption probability cannot reach 1.0 with electrons impinging on a planar detector due to electron backscatter.

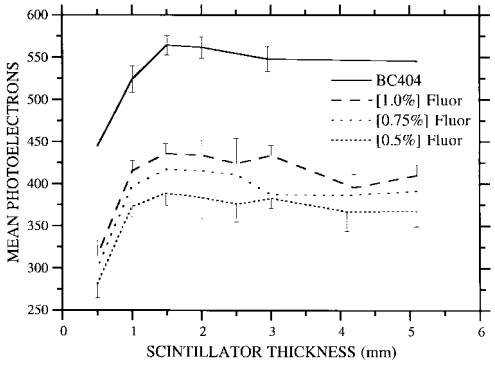

Fig. 8. Measured light output with decreasing thickness of various concentration samples compared to BC404, with the scintillators coupled directly to the PMT.

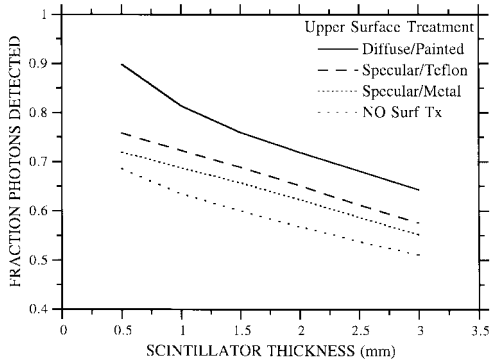

Fig. 7. Simulated light output of various thickness plastic scintillators in contact with a glass faceplate PMT. Various surface treatments were simulated for the upper surface; all conditions had roughened, absorbing sides.

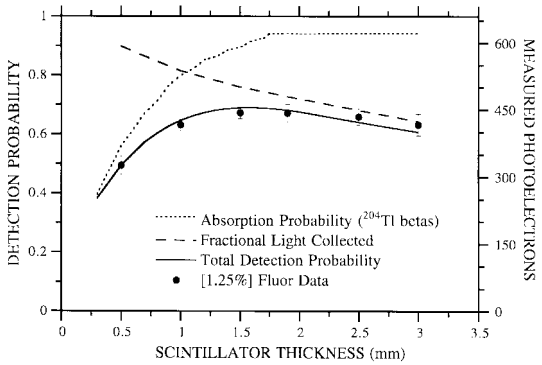

Fig. 9. Measured light output compared to simulation results. The product of simulated absorption probability and light output gives the total detection probability in the measurement configuration. Note the good fit between simulation and measured data for the 1.25% scintillator for these thicknesses.

E. Measured Geometrical Effects

The measured light output as a function of scintillator thickness results are shown for weighted means of ^{204}Tl irradiation (Fig. 8). Scintillators above the 1.0% fluor concentration had identical trends as the 1.0% scintillator for various thicknesses and did not grossly deviate from the concentration trends (Fig. 5). Although similar trends with thickness were observed with the ^{207}Bi irradiated samples, the spectral characteristics degraded near 1.0 mm thicknesses (see Section III-F). Measurements with BC404 disks coupled to front-end fiber optics, as in the intended imaging device, showed identical trends in light output with thickness [5].

The light output was observed to have little variation as a function of scintillator thickness down to $\sim$1.5 mm (Fig. 8). At 1.5 mm thickness, the electron trajectory simulation predicted 89% absorption of ^{204}Tl betas in plastic, which is very near the predicted 94% total absorption for thick disks (Fig. 9 and [5]). The product between the simulated energy deposition and light output for plastic scintillators reached a maxima near 1.5 mm for measured ^{204}Tl beta continua (Fig. 9). This trend is expected to be similar for ^{18}F positrons of similar energy. There were larger deviations between simulations and measurements for $>$3 mm scintillators (Fig. 9, not shown), but simulations indicated that the light spread in these scintillators detrimentally affected the imaging ability [4].

The 1.5 mm thickness $\times$ 1.25 cm ϕ plastic scintillating disk detector has ideal geometry for the imaging device. Less than 1.5 mm, incomplete energy deposition dominates increasing light output as measured and predicted by simulations, and thinner disk scintillators may thus be less effective for the imaging device. These results also agree with measurements of plastic disk scintillators on fiber optics [5].

F. Thin Scintillator Response

For thin detectors ($<$2.0 mm), asymmetric peaks were observed at low energies for all plastic scintillators tested in this work with ^{207}Bi conversion electrons and ^{204}Tl betas (Fig. 10). These peaks arise from the most probable energy loss from electrons traversing a medium (Landau distribution). The most probable energy loss is at the peak of the distribution, with the mean energy loss of incident electrons displaced to the high energy side, due to the long high energy exponential tail [14], [15].

Provided that a thin scintillator is utilized, and that low enough thresholds can be attained with sufficient light transfer through 2 m of optical fibers in the beta imaging device, the Landau peak can potentially be used as an energy calibration point in otherwise featureless spectra. Further investigations will be undertaken to more clearly understand the applicability of the Landau distribution for energy calibration. Back-

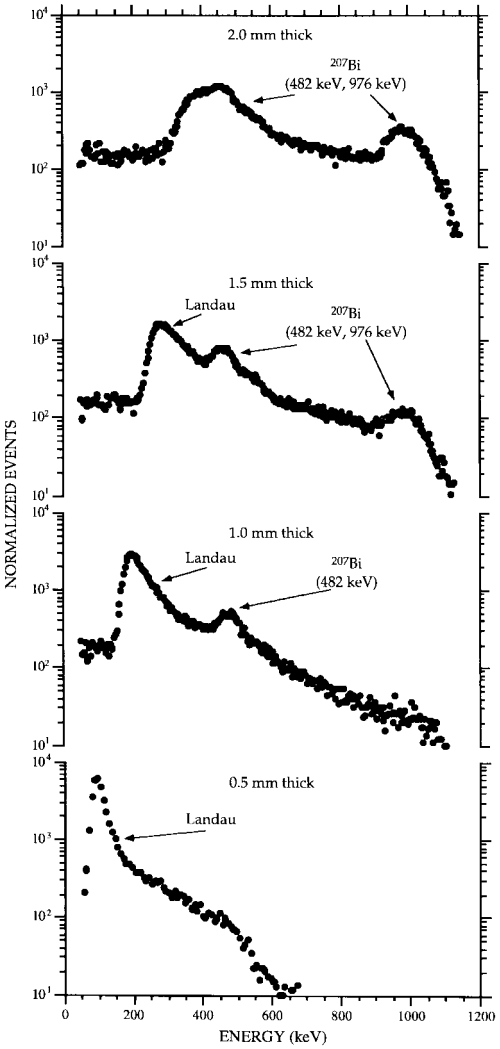

Fig. 10. Spectral response of four [1.0%] thin scintillators to ^{207}Bi irradiation. Note the disappearance of the conversion electron peaks as the scintillator thickness, thus absorption efficiency, decreases.

scattered Compton edge electrons from gamma interactions, which produce a distinct peak at the Compton edge, have also been investigated for energy calibration with thin plastic scintillators [3]. Unfortunately, poor gamma efficiencies in detectors that are ideal for beta imaging make backscatter calibration methods difficult.

The background contribution results indicate that for very thin, low density scintillators the attenuation of gammas varies linearly with thickness (Fig. 11). This result corresponds well to narrow beam geometry attenuation calculations for thin plastics.

IV. Discussion and Conclusion

The ideal continuous disk detectors for use in the intraoperative beta imaging device should have the following characteristics: 1) high light output (facilitated by various external reflectors); 2) good spectral match with the photodetector of choice; 3) low density and low Z; 4) minimal thickness; and 5) good time decay characteristics for the expected *in vivo* count rates. Despite similar beneficial characteristics of the

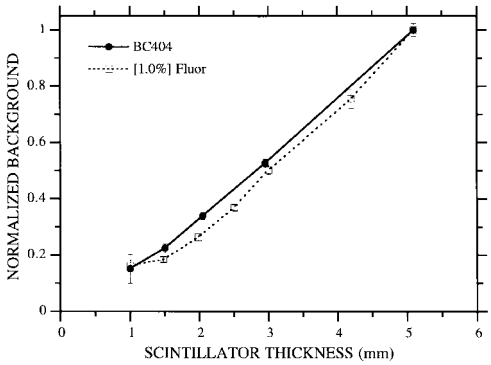

Fig. 11. Gamma background contribution normalized to the 5-mm-thick scintillator measurements.

new plastic scintillator(s) compared to the existing BC404, e.g., low density leading to low background, fast time decay properties (<2 ns, useful in fast counting or short half-life isotope measurement experiments), and similar spectral emission characteristics (~433 nm, well matched to bialkali PMT's), the 30% lower light yield precludes use of this new scintillator in the anticipated low light level situation with fiber optics and PMT photodetectors. Several factors have been identified, however, as beneficial to scintillation detector optimization for the imaging detector.

Increasing fluor concentration did demonstrate improved light output in these new organic scintillators. Perhaps increasing the dopant concentration in currently available high light output scintillators (e.g., BC404) may improve light output characteristics even further. As thin scintillators (<3 mm) are needed to minimize background, self-absorption of scintillation light is minimized while light output is maximized.

Monte Carlo simulations of energy deposition and light collection accurately predicted the optimum scintillator thickness for maximum signal detection probability as compared with measurements. As the scintillator thickness decreased, the slowly increasing detection probability increased until a roll-off at 1.5 mm, where poor (decreased) energy deposition began to dominate the light collection. Simulations indicate that this thickness of plastic scintillator is expected to have good spatial resolution properties as well.

Energy calibration with centroids of beta continua was shown to correlate with monoenergetic electron responses. A potential method of energy calibration with Landau distributions observed in the energy spectra of the thin samples was also identified.

General plastic disk scintillator properties and characteristics were identified for use with a beta imaging intraoperative probe. These characteristics will be exploited during the ongoing imaging detector optimization.

Acknowledgment

The authors would like to thank Dr. M. Kusner, Dr. J. Barrio, Dr. Y. Shao, and Dr. E. Reisler for helpful discussions, and P. Cheung, K. Meadors, and G. Moffat for expert technical assistance.

REFERENCES

[1] L. R. MacDonald *et al.*, "Investigation of the physical aspects of beta imaging probes using scintillating fibers and visible light photon counters," *IEEE Trans. Nucl. Sci.*, vol. 42, no. 4, pp. 1351–1357, 1995.

[2] M. P. Tornai *et al.*, "Development of a small area beta detecting probe for intra-operative tumor imaging," *J. Nucl. Med.*, vol. 36, no. 5, p. 109, 1995.

[3] L. R. MacDonald *et al.*, "Small area, fiber-coupled scintillation camera for imaging beta-ray Distributions Intraoperatively," in *Proc. SPIE: Photoelectronic Detectors, Cameras & Systems*, 1995, vol. 2551 pp. 92–101.

[4] M. P. Tornai *et al.*, "Design considerations and initial performance of a 1.2 cm^2 beta imaging intra-operative probe," *IEEE Trans. Nucl. Sci.*, vol. 43, no. 4, pp. 2326–2335, 1996.

[5] C. S. Levin *et al.*, "Optimizing light output from thin scintillators used in beta-ray camera for surgical use," *IEEE Trans. Nucl. Sci.*, vol. 43, no. 3, pp. 2053–2060, 1996.

[6] E. Tanaka, T. Hiramoto, and N. Nohara, "Scintillation cameras based on new position arithmetics," *J. Nucl. Med.*, vol. 11, no. 9, pp. 542–547, 1970.

[7] J. B. Birks, *Theory and Practice of Scintillation Counting.* Oxford: Pergamon, 1970.

[8] A. D. Bross, A. Pla-Dalmau, and C. W. Spangler, "New fluorescent compounds for plastic scintillator applications," *Nucl. Instrum. Methods*, vol. A325, pp. 168–175, 1993.

[9] L. M. Bollinger and G. E. Thomas, "Measurement of the time dependence of scintillation intensity by a delayed-coincidence method," *Rev. Sci. Instr.*, vol. 32, no. 9, pp. 1044–1050, 1961.

[10] J. P. O'Callaghan, R. Stanek, and L. G. Hyman, "On estimating the photoelectron yield and the resultant inefficiency of a hotomultiplier-based detector," *Nucl. Instrum. Methods*, vol. 225, no. 1, pp. 153–163, 1984.

[11] M. Moszynski and B. Bengtson, "Light pulse shapes from plastic scintillators," *Nucl. Instrum. Methods*, vol. 142, pp. 417–434, 1977.

[12] B. Leskovar and C. C. Lo, "Single photoelectron time spread measurement of fast photomultipliers," *Nucl. Instrum. Methods*, vol. 123, pp. 145–160, 1975.

[13] G. F. Knoll, T. F. Knoll, and T. M. Henderson, "Light collection in scintillating detector composites for neutron detection," *IEEE Trans. Nucl. Sci.*, vol. 35, no. 1, pp. 872–875, 1988.

[14] L. Landau, "On the energy loss of fast particles by ionization," *J. Phys.*, vol. 8, no. 4, pp. 201–205, 1944.

[15] M. Aderholz, I. Lehraus, and R. Matthewson, "Reduction of the ionization loss distribution width of several simultaneous relativistic particles traversing a scintillation counter," *Nucl. Instrum. Methods*, vol. 123, pp. 45–50, 1975.